Numerical analysis of a 3D radially symmetric grain attached to a free crystal surface

Jacob Kanel[1], Amy Novick-Cohen[1], Arkady Vilenkin[2]

[1] *Department of Mathematics, Technion-IIT; Haifa 32000, Israel*
[2] *The Racah Institute of Physics, The Hebrew University of Jerusalem; Jerusalem 91904, Israel*

Abstract

1 Abstract

We study a 3D bicrystal containing an axially symmetric shrinking grain which is initially a spherical segment attached along a circular groove root to the flat exterior surface of the second grain. Following Mullins [1]-[3], a time dependent problem is formulated for the coupled motion of the grain boundary, the groove root, and the external surface. Numerical solutions calculated using an implicit finite difference scheme indicate that the grain shrinks and disappears in finite time, no non-trivial limiting motion is seen, and there is no pinning of the grain boundary that might be associated with so called "jerky motion." Surprisingly enough, the surface groove seems to only minimally affect the grain boundary motion, the groove depth varies non-monotonely in time, and after annihilation of the grain, the exterior surface has a profile which depends on the system's history and contains certain features which can be interpreted as so called "ghost lines."

Key words: Grain boundaries, grain growth, surface diffusion, theory.

2 Introduction

The influence of the exterior crystal surface on grain growth dynamics has been discussed extensively since the middle of the last century. Mullins [3] proposed that groove roots could serve as anchors for moving grain boundaries and could give rise to non-monotone or "jerky" motion of the grain boundaries. Mullins' conjecture gave rise to considerable interest in the investigation of

coupled surface and interface motion. Although many experiments have been done in this direction, we do not know of any experimental paper which shows explicitly the phenomenon of "jerky" motion in a one component system. The recent investigation [4] showed that under typical conditions, the surface groove in Al minimally affects grain boundary motion. In [5] it was shown theoretically that in the quarter loop geometry, the grain groove has very little effect on the kinetics of grain boundary migration for typical values of the parameters, but that it may even accelerate migration in very special cases. In none of the theoretical papers that considered coupled grain boundary surface groove motion in two dimensional geometries such the quarter loop and Sun-Bauer geometries [5] - [11] was any trend to non-monotone motion seen. [1]

Nevertheless, it is known that the exterior crystal surface can sometimes strongly influence the motion of the interface. For example, grain boundary migration driven by anisotropy of the exterior surface has been reported in [3,14,15]. In the last of these three papers, it is shown that an increase of the driving force in such systems can induce a decrease in the velocity of the grain boundary. Another example of surface driven grain boundary migration is presented in [16] where grain growth in a one dimensional polycrystalline array occurs via interaction of the surface grooves. Strong influence of the external surface on the interfacial motion is shown in [17] where the presence of a grain groove gives rise to a second velocity of steady motion.

The short review given above shows that the problem of coupled surface-interface motion is intriguing, and whether or not jerky motion can occur in one-component systems still remains an open question. Note that all of the literature which has been cited deals with special geometries where the systems being described have a uniform cross-section and are hence effectively two dimensional, and this simplifies the analysis considerably. In the present paper we consider a 3D axisymmetric geometry. This geometry, while still simple, is closer than the uniform cross-sectional systems to modelling true 3D motion. Therefore it is not surprising that new effects are seen here which probably give some hint as to what can be seen in arbitrary 3D geometries.

Typical experimental data for grain boundary migration usually contains information about the speed or the position of the groove root as a function of time, and nothing about the nature of the grain boundary's shape which determines the driving force of the process. In some special cases, such as the "quarter loop" or the "Sun-Bauer" geometry, the shape of the grain boundary can be calculated analytically. However in these cases no interesting non-monotone behavior was observed in one component systems. Hence it seems interesting to investigate numerically the behavior of a system in the context

[1] Some theoretical results in this direction have been reported [12,13], but they can be dismissed rather easily.

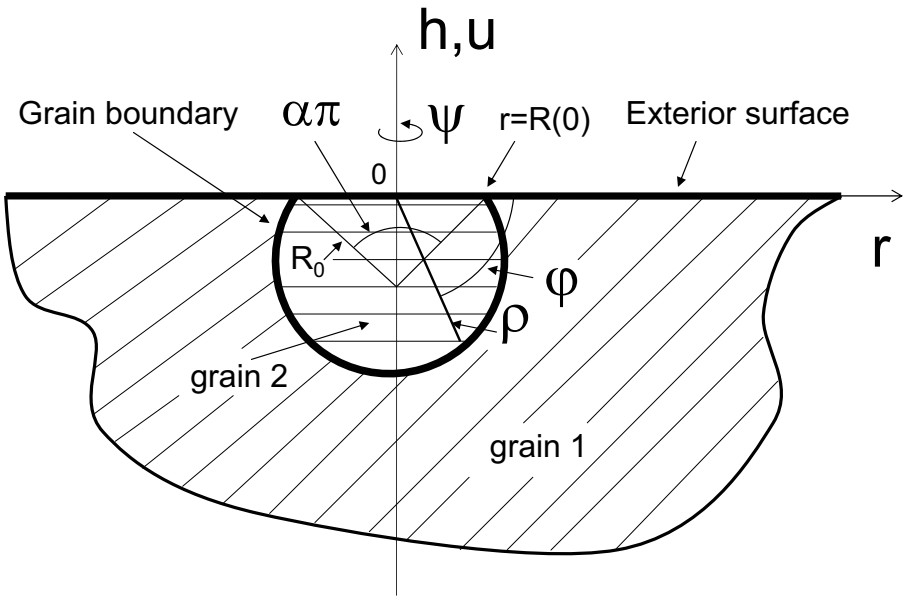

Fig. 1. A schematic cross-section of the bicrystal.

of a somewhat non-traditional configuration. We focus here on a system in which the initial grain is of the form of part of a sphere. This is a very idealized case, and probably difficult if not impossible to realize in experiment. However, as we shall see, this system exhibits rather complicated dynamics and should help in extending our understanding of the external surface - grain boundary interaction in general. Our numerical analysis indicates that the evolution of the system is dominated by transients that lead to rather complicated surface morphology even in the isotropic case. The driving force for the evolution of the system is the reduction of surface and grain boundary energies. We have calculated both the grain boundary and exterior surface energies as a function of time, and found that the grain boundary energy seems effectively uninfluenced by its interaction with the surface via the groove root and varies much as it would for a freely moving grain boundary. The energy of the external surface corresponds initially to that of a flat external surface, then increases, reaching some maximal value just prior to the vanishing of the grain and its grain boundary, and then decays, with relaxation continuing after the disappearance of the grain. We note that initially, for typical values of the system parameters, the grain boundary energy in a bicrystalline geometry is an order of magnitude larger than the external surface energy. When the grain has shrunken and become very small, the two energies are of the same order of magnitude. But the smallness of the grain implies that its curvature is very large, and so the grain can be expected to continue to shrink very rapidly due to its high curvature, and no pinning or related instability is thus to be expected to occur in a one component isotropic system.

3 The Equations for Coupled Surface and Grain Boundary Motion in an Axisymmetric Geometry

Surface diffusion and motion by mean curvature

For our initial conditions, we shall consider a bicrystal in which one grain which constitutes a segment of a sphere is embedded within a second grain of infinite extent. More specifically, the external surface shall be assumed to be initially flat and the grain boundary will be taken to be initially in the form of a spherical segment which can be described in terms of an angle, $\alpha\pi$, and an initial radius, R_0, see Fig. 1. Since the bicrystal is in a geometry in which the exterior surface and the grain boundary are initially axially symmetric, we shall look for axially symmetric solutions which, when described in terms of the cylindrical coordinate system, will be independent of the polar angle variable, Ψ, see Fig. 1. Thus, the evolution of our system can be described in terms of the variables $h(r,t)$, $u(r,t)$, and $R(t)$, where $h(r,t)$ and $u(r,t)$ denote respectively the heights of the exterior surface and of the grain relative to the height of the exterior surface at $\pm\infty$ where it shall be assumed to remain flat, and $R(t)$ denotes the radius of the circular groove as a function of t.

Taking the motion of the exterior surface to be governed by surface diffusion:

$$V_n = B\triangle_s\mu, \quad \mu = -\kappa,$$

where V_n is the normal velocity, $\triangle_s$ is the surface Laplacian, κ is twice the mean curvature, μ denotes the chemical potential, and B is constant, and taking the motion of the grain boundary to be governed by motion by mean curvature:

$$V_n = A\kappa,$$

where V_n denotes the normal to the surface, κ denotes twice the mean curvature, and A is constant, for both surfaces it is necessary to calculate the mean curvature. Because of the axial symmetry of the system, the principal directions to the exterior surface and the grain boundary are given by a) the tangent to the surface which points in a constant azimuthal direction, and b) the tangent to the surface which points in a direction of constant r. Thus the principal curvatures for the exterior surface are given by a) $h_{rr}(1+h_r^2)^{-3/2}$ and b) $(h_r/r)(1+h_r^2)^{-1/2}$, and therefore

$$\kappa = \frac{h_{rr}}{(1+h_r^2)^{3/2}} + \frac{h_r}{r\sqrt{1+h_r^2}} = \frac{1}{r}\left[\frac{rh_r}{\sqrt{1+h_r^2}}\right]_r.$$

Since the mean curvature depends only on r, $\triangle_s\mu = \mu_{ss}$, where $\partial_s = (1+h_r^2)^{-1/2}\partial_r$. Noting that the normal velocity along the exterior surface may be

expressed as $V_n = h_t(1+h_r^2)^{-1/2}$, it follows from the discussion above that the equation of motion for the exterior surface may be written as

$$h_t = B\left[\frac{\mu_r}{\sqrt{1+h_r^2}}\right]_r. \tag{1}$$

From the equation for motion by mean curvature and the discussion above, it follows readily that

$$u_t = A\left[\frac{u_r}{r} + \frac{u_{rr}}{1+(u_r)^2}\right]. \tag{2}$$

If, however, the parameter α (see Fig. 1) is less then one, then the grain boundary shape $u(r,t)$, at least initially and at early times, is not single valued. To sidestep this difficulty, instead of expressing the equation of grain boundary motion in radial coordinates, we introduce polar coordinates (ρ,φ), and the origin of the polar coordinate system is taken to coincide with the origin of the radial coordinate system, see Fig. 1. In terms of this new coordinate system, we may set $u(r,t) = \rho(\varphi,t)\sin\varphi$, where $r = \rho(\varphi,t)\cos\varphi$ and $-\pi/2 \leq \varphi \leq \phi(t)$, where $\varphi = \phi(t)$ demarcates the location of the groove root. In the problem formulation which follows shortly, the equation of motion for the grain boundary will be given explicitly in terms of $\rho = \rho(\varphi,t)$, φ, and $\phi(t)$.

The problem formulation

To complete the problem formulation, boundary conditions must be prescribed. The basic physical laws governing the boundary conditions at the tri-junction line which occurs along the groove root were understood and explained by Mullins in [3], although presented there only in a linearized form. Following the discussions in [3,5,9], we take the tri-junction line to be governed by Young's law [18,2] which expresses a balance of mechanical forces, continuity of the chemical potential, and balance of mass flux. In terms of the notation introduced above, these conditions are to be imposed at $r = R(t)$ and at $\varphi = \phi(t)$. As mentioned previously, the external surface h will be taken to be asymptotically flat. This far field condition reflects the assumption that sufficiently far away from the grain groove, the effect of the grain boundary on the overall height of the specimen is negligible. Additional boundary conditions are needed along the axis of symmetry where $r = 0$ and $\varphi = -\pi/2$, to reflect the assumed symmetry of the system. In summary, we may write our problem formation as

$$
(\mathbf{P})\quad\begin{cases}
h_t = B\Big[\frac{\mu_r}{\sqrt{1+h_r^2}}\Big]_r, \quad \mu = -\frac{1}{r}\Big[\frac{rh_r}{\sqrt{1+h_r^2}}\Big]_r, \quad 0<r<\infty, \quad r\neq R(t), \quad t>0,\\
\rho\rho_t = A\Big[-2-\Big(\frac{\rho_\varphi}{\rho}\Big)\tan\varphi+\Big(\frac{\rho\rho_{\varphi\varphi}-\rho_\varphi^2}{\rho^2+\rho_\varphi^2}\Big)\Big], \quad -\frac{\pi}{2}<\varphi<\phi(t), \quad t>0,\\
\phi(t) = \arctan[h(R(t),t)/R(t)], \quad t>0,\\
\rho(\phi(t),t) = \sqrt{h^2(R(t),t)+R^2(t)}, \quad t>0,\\
h(R(t)+0,t) = h(R(t)-0,t) = \rho(\phi(t),t)\sin\phi(t), \quad t>0,\\
h_r(0,\,t) = 0, \quad t>0,\\
\mu_r(0,\,t) = 0, \quad t>0,\\
\rho_\varphi(-\frac{\pi}{2},\,t) = 0, \quad t>0,\\
\arctan h_r(R(t)+0,\,t) - \arctan h_r(R(t)-0,\,t) = 2\arcsin(m/2), \quad t>0,\\
\arctan h_r(R(t)+0,\,t) + \arctan h_r(R(t)-0,\,t) = \pi + 2\arctan\Upsilon(t),\\
\qquad \text{where } \Upsilon(t) = \Big[\frac{\rho_\varphi(\phi(t),t)\tan\phi(t)+\rho(\phi(t),t)}{\rho_\varphi(\phi(t),t)-\rho(\phi(t),t)\tan\phi(t)}\Big], \quad t>0,\\
\mu(R(t)+0,t) = \mu(R(t)-0,t), \quad t>0,\\
\frac{\mu_r}{\sqrt{1+h_r^2}}\big|_{r=R(t)-0} = \frac{\mu_r}{\sqrt{1+h_r^2}}\big|_{r=R(t)+0}, \quad t>0,\\
h(\infty,\,t) = 0, \quad t>0,\\
h_r(\infty,\,t) = 0, \quad t>0.
\end{cases}
$$

The first and second equations describe respectively the motion by surface diffusion of the exterior surface and the motion by mean curvature of the grain boundary. Note that we are working here with a full nonlinear formulation and not with the small slope linearized approximation which has traditionally been employed. The third, fourth, and fifth equations describe the geometric conditions which must hold at the groove root if the basic configuration in which the grain boundary is attached to the exterior surface at the groove root is to persist over time. The next three equations constitute conditions at the origin reflecting the assumed axial symmetry. The next four conditions, conditions nine though twelve, give the physical boundary conditions which have been assumed to hold at the groove root; the first two of these conditions express Young's law at the triple junction line, and the latter two of these conditions express continuity of the chemical potential and a balance of mass flux. In Young's law, $m = \gamma_{\text{grain boundary}}/\gamma_{\text{exterior surface}}$ is the ratio of the

external surface to grain boundary energies. The last two equations reflect the assumption that the exterior surface is asymptotically flat far away from the embedded grain.

Further insight into this system can be gained by considering [11] where the governing equations are given in terms of coordinate free geometric quantities. We note that closely related systems have also recently been obtained in a sharp interface limit from a system of Allen-Cahn/Cahn-Hilliard equations [19] and from a phase field model for electromigration of intergranular voids [20].

3.1 Parameters

Problem (P) contains 3 physical parameters and 2 geometric parameters which reflect the initial conditions. The physical parameters are A, the kinetic coefficient in the equation for grain boundary motion, B, the mobility coefficient in the equation for surface evolution, and m, the ratio of the external surface to grain boundary energies which appears in Young's law. Note that $[A] = \mathrm{cm}^2/\,\mathrm{sec}$, $[B] = \mathrm{cm}^4/\,\mathrm{sec}$, and $[m] = 1$. The geometric parameters consist of α, which prescribes the proportion of the sphere determining the initial grain shape, and R_0, the initial radius of the grain, see Fig. 1. Note that $[\alpha] = 1$ and $[R_0] = \mathrm{cm}$.

The parameters, A and B may be used in defining $L = \sqrt{B/A}$ as a unit of length, and $\theta = B/A^2$ as a unit of time. Since typically $B \simeq 10^{-20}\,\mathrm{cm}^4/\,\mathrm{sec}$ and $A \simeq 10^{-6} - 10^{-12}\,\mathrm{cm}^2/\,\mathrm{sec}$, it follows that typically $L \simeq 10^{-6} - 10^{-4}\mathrm{cm}$ and $\theta \simeq 10^{-8} - 10^{4}\,\mathrm{sec}$. Setting $t \to t/\theta$ and $r \to r/L$, and subsequently $h(r,t) \to h(r,t)/L$, $\rho(\varphi,t) \to \rho(\varphi,t)/L$, $R(t) \to R(t)/L$, and $R_0 \to R_0/L$, a dimensionless formulation of Problem (P) is obtained. The dimensionless formulation, which for simplicity we shall not write out explicitly, can be written out in terms of three dimensionless parameters: α, R_0, and m.

4 The Numerical Procedure

Suppose that the solution is known up to time t for some $t > 0$, and suppose that we use the past values of $R(t)$ to approximate $R(t + \triangle t)$, for some fixed $\triangle t > 0$. Taking $R(t + \triangle t)$ to now be known, we can use the equations in Problem (P) to approximate $h(r,\, t + \triangle t)$ and then $u(r,\, t + \triangle t)$. This can be accomplished by first solving a "surface problem" for $h(r,\, t + \triangle t)$ using finite differences based on the equations for surface diffusion and the boundary conditions in (P) which dependent on h and μ only. Having approx-

imated $h(r,\, t+\triangle t)$, an approximation for the value of $u(R(t+\triangle t),\, t+\triangle t)$ or equivalently $\phi(t+\triangle t)$, $\rho(\phi(t+\triangle t), t)$ is implied by the persistence boundary condition. The values of $\phi(t+\triangle t)$, $\rho(\phi(t+\triangle t), t)$, the boundary condition $\rho_r(0,\, t+\triangle t) = 0$, and the equation for grain boundary motion together constitute a "grain boundary problem" whose solution by a finite difference scheme gives an estimate of $u(r,\, t+\triangle t)$. By now, all of the equations and boundary conditions in Problem (P) have been used, except for the second boundary condition from Young's law which connects $h_r(R(t+\triangle t),\, t+\triangle t)$ with $\rho(\phi(t+\triangle t))$ and $\rho_\varphi(\phi(t+\triangle t),\, t+\triangle t)$. This last condition can be used to correct our initial approximation of $R(t+\triangle t)$. The process can be iterated until sufficient accuracy is achieved. Implicit finite difference schemes are used at each step to solve the "surface" and "grain boundary" problems.

We remark that while the initial conditions have been taken in accordance with the geometry prescribed by Fig. 1 and described above, Young's law has been imposed at the groove root on the finest finite difference scale for the sake of compatibility.

5 Numerical Results

Solutions were calculated for several sets of initial data and parameter values. The initial data is determined here by the initial shape of the grain, which is taken as a spherical segment which can be prescribed by an angle, $\alpha\pi$, and a (non-dimensional) radius, R_0. See Fig. 1. Note that if $\alpha = 0$, then initially the embedded grain is a sphere, and if $\alpha = 1$, then initially it is a hemisphere. We have investigated initial data with $\alpha = 0.1, 0.4, 1$, and $R_0 = 10^2, 10^3, 5\times 10^3, 10^4$. The only additional parameter which needs to be fixed is m, which we have taken as $m = 0.1, 0.3, 0.5, 1$. For all tested values of the parameters, the behavior of solutions was seen to be relatively similar except that when $\alpha < 1$, the groove root motion was non-monotone and changed directions as the grain shrank. The typical features of the dynamics are summarized below.

The case $\alpha = 1$ in which the initial shape is hemispherical constitutes a special case in which the grain boundary meets the exterior surface at 90°, and if $m = 0$ the exterior surface will remain flat, no groove root will form, and the grain will remain hemispherical as it shrinks. In this case, its radius can easily be shown to be given by $R(t) = \sqrt{R^2(0) - 4t}$. This special case can be used as a basis for comparison for other solutions in order to see the degree to which the grain boundary motion is effected by the groove root and the exterior surface. Such a comparison is given with $\alpha = 1$ for $R_0 = 100, 10000$, and $m = 0.3, 1$, in Fig. 2 where the data are presented in rescaled coordinates. It can be seen that the overall motion of grain boundary seems only slightly

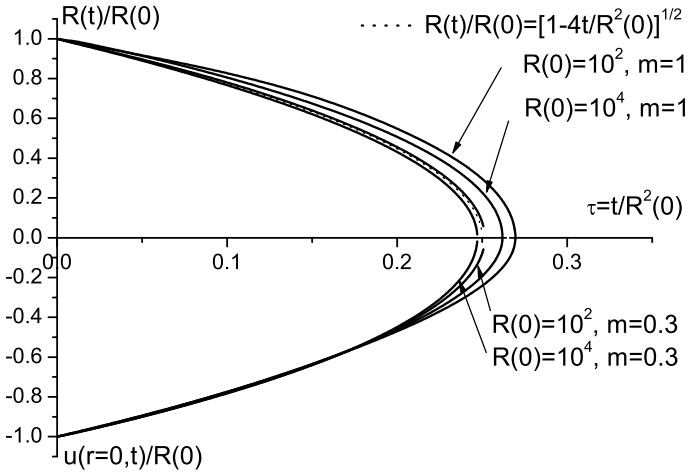

Fig. 2. The variation in the grain size as a function of time is given by the solid line. The dashed line shows the kinetics of freely moving grain boundary. The data are presented in rescaled coordinates. Note that $u(r = 0, t)$ corresponds to the height of the lowest point of the grain boundary.

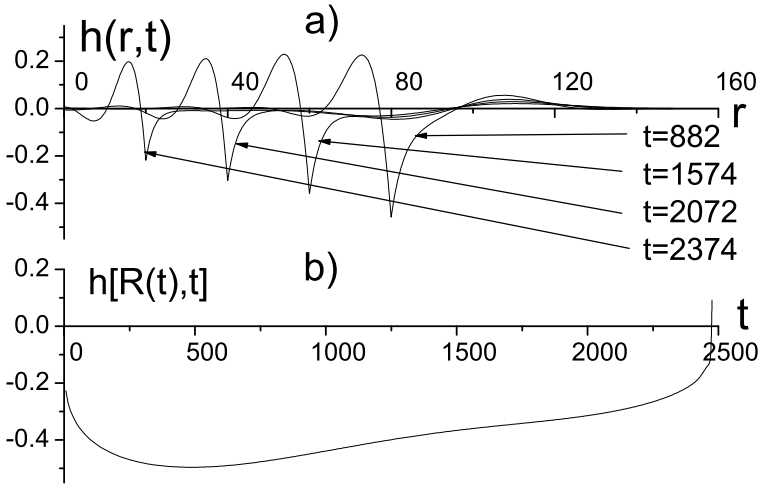

Fig. 3. a) The shape of the exterior surface at various times. b) The dependence of the groove depth as a function of time. Here $\alpha = 1$, $R_0 = 100$, and $m = 0.3$.

affected by the interaction with the exterior surface for $m < 0.3$.

The central cross-section of the exterior surface at different times and the groove root depth as a function of time are presented for this simulation in Fig. 3a and Fig. 3b, respectively. It can be seen here that the groove root moves continuously towards the origin (see Fig. 2) and that the groove root depth has a minima in time. The exterior surface profile seems to "remember some history" in that a small indentation or valley forms in the exterior surface at around $r = 80$ which persists up to and past the time that the grain disappears. This indentation appears to form about when $t \approx 500$, just after the groove root has crossed this position. At this time, the groove depth can be seen to have a minimum, see Fig. 2. Even though such a feature can be explained

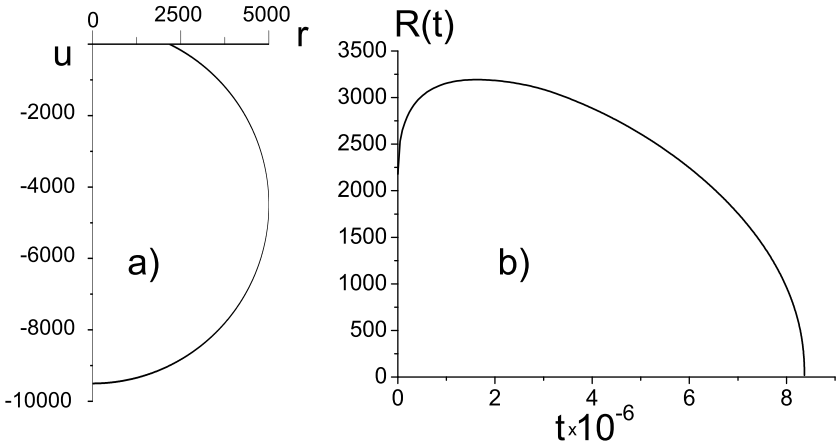

Fig. 4. a) The central cross-section of the initial grain. b) The groove root's position as a function of time. Here $\alpha = 0.1$, $R_0 = 5 \times 10^3$, and $m = 0.1$.

as simply a transient of the evolution, it could also be easily interpreted as a "ghost line" from which a grain boundary had detached. No "pinning", or delay in the groove root displacement was observed, see Fig. 2.

In a simulation in which $\alpha = 0.1$, $R_0 = 5 \times 10^3$, and $m = 0.1$, the groove root was seen to change its direction of motion as it progressed, see Fig. 4. Moreover, the dependence of the groove depth on time is more complicated; there are two local minima which occurred when $t \approx 2 \times 10^6$ and $t \approx 4 \times 10^6$, as well as a local maximum which occurred when $t \approx 3.2 \times 10^6$, see Fig. 5. The data in Fig. 4b indicates that these maxima and minima occurred when the groove root was already moving steadily towards the origin, and that they appear at a distance $\approx 2500 < r <\approx 3000$ from the origin, which corresponds to the region in which the "ghost line" valley appears at later times during the grain evolution, see Fig. 6. Qualitatively the same dynamics were observed when $\alpha = 0.4$ and for all of investigated sets of parameters.

The formation of a residual "valley" ("smooth groove" or "ghost line") can be explained as follows. Since m has been assumed to be small, the evolution of the exterior surface should be governed primarily by surface diffusion and should only be weakly affected by the motion of the grain boundary. Hence features along the exterior surface with a characteristic width of $\triangle r$ can be expected to relax at a rate proportionate to $(\triangle r)^4$. Noting that, for example, in Fig. 6, the valley at $r = 3000$ has a characteristic width of $\triangle r \approx 1000$ and the peak at $r = 500$ has a characteristic width of $\triangle r \approx 100$, their relaxation times should be proportional to 10^{12} and to 10^8 respectively. Therefore the valley should persist long after the peak, and thus also the grain, have disappeared.

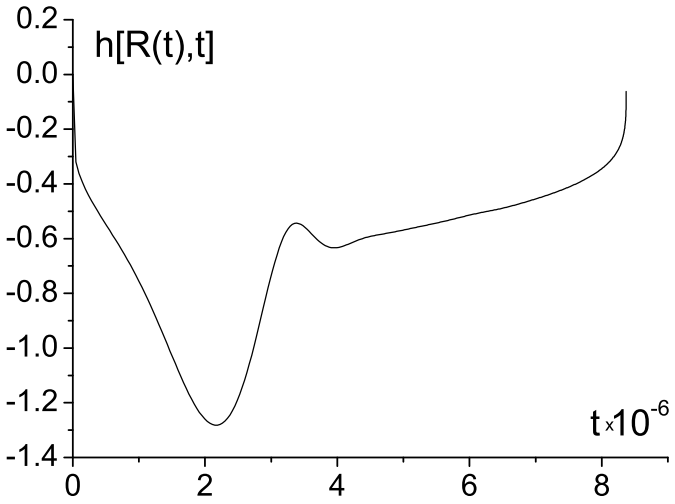

Fig. 5. The groove depth as a function of time. Here $\alpha = 0.1$, $R_0 = 5 \times 10^3$, and $m = 0.1$.

5.1 Energetics

We turn now to see what our equations imply in terms of energy. The energy here has two components, the energy of the exterior surface and the energy of the grain boundary, and it is easy to show as in [19] that the overall reduction in energy acts as the driving force for the system. We remark that the energy of the external surface, $\gamma_{\text{surface}}\, S_{\text{surface}}$, should be infinite, since S_{surface} is infinite as long as $\gamma_{\text{surface}} \neq 0$, the shrinking grain is finite, and the system extends out to infinity. However, we can express the energy of the exterior surface in terms of its energy relative to a flat exterior surface of infinite extent

$$E_{\text{surface}} = \gamma_{\text{surface}}\, \triangle S_{\text{surface}},$$

where $\triangle S_{\text{surface}}$ represents the reduced surface area, $\triangle S_{\text{surface}} := S_{\text{surface}} - S_{\text{flat surface}}$, and E_{surface}, so defined, can be expected to be finite. Note in particular that $E_{\text{surface}} = 0$ for a flat surface. Setting $E_{\text{grain boundary}} = \gamma_{\text{grain boundary}}\, S_{\text{grain boundary}}$, the total (relative) energy of the system may be expressed as

$$E_{\text{total}} = E_{\text{surface}} + E_{\text{grain boundary}}.$$

Since only the ratio $m = \gamma_{\text{grain boundary}}/\gamma_{\text{exterior surface}}$ appears in our problem formulation, it is convenient to work with the rescaled energy

$$e_{\text{total}} = E_{\text{total}}/\gamma_{\text{surface}} = \triangle S_{\text{surface}} + m\, S_{\text{grain boundary}}.$$

In terms of this definition for the system's energy, initially the value of the energy is given by the energy of the grain boundary alone since we are supposing that the exterior surface is flat at time $t = 0$, and eventually, when the grain has disappeared and the exterior surface has become flat once more, the total energy of the system should vanish. Graphs of the surface and grain boundary

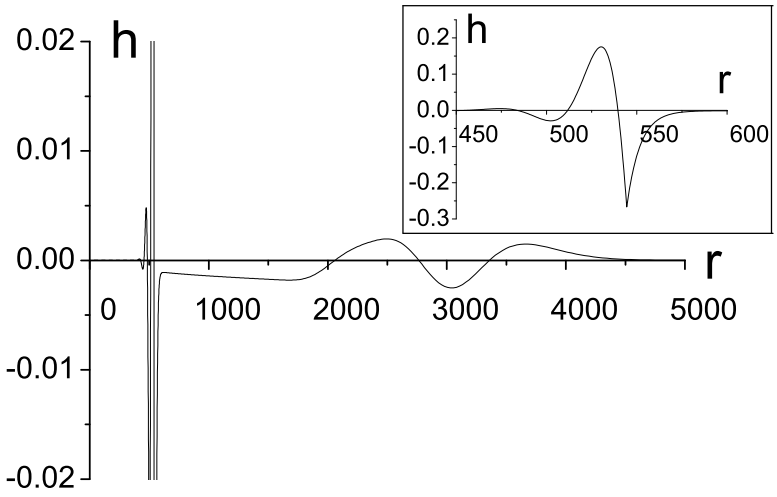

Fig. 6. The central cross-section of the exterior surface at time $t = 8.3 \times 10^6$. Here $\alpha = 0.1$, $R_0 = 5 \times 10^3$, and $m = 0.1$.

energies during a simulation with $\alpha = 0.1$, $R_0 = 5 \times 10^3$, and $m = 0.1$ are presented in Fig. 7.

At $t = 0$, the exterior surface is flat and its energy is zero, while the energy of the grain boundary appears to be maximal. The groove root starts to grow immediately, which causes the surface energy to increase at the expense of the grain boundary energy, see Fig. 7a. Nevertheless, the surface energy is so small relative to the (initial) grain boundary energy that very little deviation from the linear decrease which would be predicted for a freely moving hemispherical grain boundary can be seen in the surface energy graph (Fig. 7b). After time $t \approx 2 \times 10^6$, the groove root begins to accelerate (see Fig. 4b), and the surface energy starts to decrease. The surface energy continues to decrease up to the time at which the grain disappears. The energy of the exterior surface should continue to decrease also after the grain has disappeared, but for computational simplicity our simulations have been stopped when the grain disappears. Note that the graph of the grain boundary energy (Fig. 7b) is nearly a straight line.

6 Conclusion

The results which have been presented show that transient dynamics of coupled grain boundary migration and surface diffusion can give rise to rather complicated morphology of the external surface which can include the appearance of "ghost lines," although no pinning of grain boundary is involved in their formation. Roughly one can say that at the beginning of process, the groove depth grows for some rather short period of time until some maximal value is attained which is so large that surface diffusion cannot flatten it

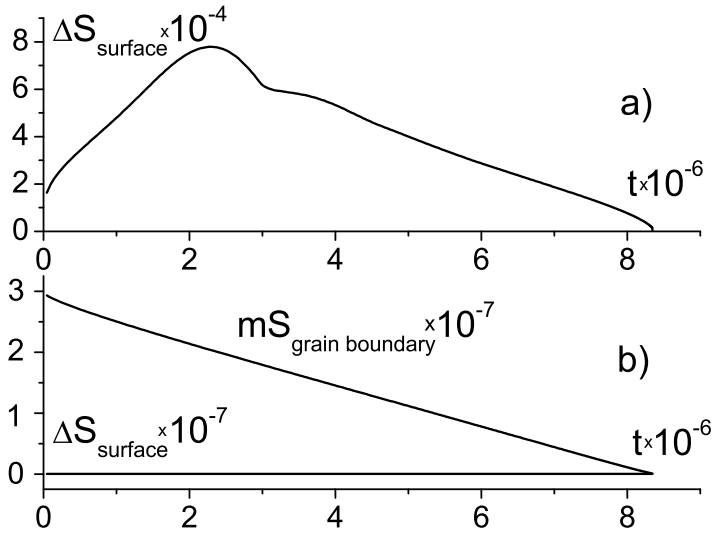

Fig. 7. a) The surface energy as a function of time. b) The surface and grain boundary energies as functions of time. They have different orders of magnitude, and it is impossible to see any variation of the surface energy on the scale of the grain boundary energy. Here $\alpha = 0.1$, $R_0 = 5 \times 10^3$, and $m = 0.1$.

out during the lifetime of the grain. One can see the imprint of this maximal groove in the surface profile even after grain annihilation. This behavior is also reflected in the evolution of the energetics of the system.

It would seem that the generation of ghost lines in real polycrystalline materials could have similar origins. In geometries where long time asymptotic solutions exist, such phenomenon cannot be expected to appear at very long times, since complete relaxation of even a deep surface groove requires only a finite amount of time. However one should expect such "ghost lines" in polycrystals where the groove roots spend a lot of time with very little displacement, since in this case the groove depth would be large and the exterior surface can be expected to continue to relax for a long time even after grain annihilation.

Acknowledgements

The authors are grateful to John W. Barrett, Xinfu Chen, and Brian Wetton for their interest, their comments, and their questions. The authors would like to acknowledge the support of the Israel Science Foundation under grant #62/02. One of the authors, A. N.-C., would like to acknowledge the hospitality of the Courant Institute.

References

[1] Mullins W. J appl phys 1956;27:900.

[2] Mullins W. J appl phys 1956;28:333.

[3] Mullins W. Acta metall 1958;6:414.

[4] Ivanov VA, Molodov DA, Shvindlerman LS, Gottstein G. Acta mater 2004;52:969.

[5] Kanel J, Novick-Cohen A, Vilenkin A. Acta mater 2003;51:1981.

[6] Min D, Wong, H. Acta mater 2002;50:5155.

[7] Zhang H, Wong H. Acta mater 2002;50:1983.

[8] Zhang H, Wong H. Acta mater 2002;50:1995.

[9] Kanel J, Novick-Cohen A, Vilenkin A. Defect and diffusion forum 2002;216-2:299.

[10] Kanel J, Novick-Cohen A, Vilenkin A. Nonlinear anal tma, 2004;59:1267.

[11] Kanel J, Novick-Cohen A, Vilenkin A. Adv diff eqns 2004;9:299.

[12] Aristov V, Fradkov V, Shvindlerman L. Phys met metall 1978;45:997 (in Russian).

[13] Hackney S. Scripta mater 1996;34:1021.

[14] Sun B, Suo Z. Acta mater 1997;45:4953.

[15] Kris R, Vilenkin A, Brokman A. J appl phys 1997;81:6723.

[16] Vilenkin A, Kris R, Brokman A. J appl phys 1997;81:238.

[17] Brokman A, Kris R, Mullins W, Vilenkin A. Scripta mater 1995;32:1341.

[18] Bailey GLJ, Watkins HC. Proc. Phys. Soc., 1950;B63:350.

[19] Novick-Cohen A. Physica D, 2000;137:1.

[20] Barrett J, Garcke H, Nürnberg R. preprint.